

# A 3-D Computational Fluid Dynamic Model to Enhance Efficiency and Predict NO<sub>x</sub> Formation in Once-Through Steam Generators

Ehsan Askari, Sr. CFD Analyst, AP Dynamics, Calgary, AB

Arthur Maesen, CFD Analyst, GDTech, Liege, Belgium

Mario Forcinito\*, Chief Technology Officer, AP Dynamics, Calgary, AB  
[mario.forcinito@ap-dynamics.net](mailto:mario.forcinito@ap-dynamics.net)

Laurent Fitschy, Lead of CFD Department, GDTech, Liege, Belgium

## **Abstract:**

*Based on our previous experience with industrial sized OTSGs, a new NO<sub>x</sub> solver as well as an LES model developed for OpenFOAM are presented, and their accuracies assessed through the case studies involving two experimental-scaled combustors. First, the validation of the CFD model was carried out using experimental data for NO<sub>x</sub> composition and heat fluxes obtained from a semi-industrial experimental combustor. Then, the acoustical waves potentially induced by the combustion process was reconstructed for a pre-mixed combustor based on information extracted from the mean flow and turbulence quantities. The objective of this final analysis is to further identify the nature of mechanisms generating these acoustical waves as well as predict their propagation inside the combustor.*

Keywords: Combustion, NO<sub>x</sub> Formation, Combustion-Induced Vibrations, Computational Fluid Dynamics (CFD)

## **Introduction**

As environmental regulations have become more stringent in terms of pollutant emissions over the years, the design of the burners must include considerations to ensure high combustion efficiency while meeting pollution control standards during operation. In most industrial applications, low-NO<sub>x</sub> staged burners are commonly employed due to its capability to reduce emissions at relatively low costs. Such

burners usually rely on fuel staging as the main mechanism to lower the NO<sub>x</sub> contents in the flue gas. Feeding the fuel at different stages, progressively release the heat of reaction and reduce the overall flame temperature leading to minimum NO<sub>x</sub> generation. In addition to recirculation zones created by the fuel staging, dilution of the reacting mixture can also be achieved in burners equipped with Flue Gas Recirculation (FGR) system. This technique allows part of the flue gas to be drawn inside the burner and mixed with combustion air. As the reacting mixture becomes diluted, the net rate of formation of NO<sub>x</sub> compounds decreases. A somewhat neglected design constraint is that the mechanical/structural parts added to burner for NO<sub>x</sub> reduction purposes, e.g., FGR, are prone to vibrations issues. The combined effects of compressibility, heat release during combustion reactions and turbulence induce the vibrations. This is of particular concern with larger size OTSG where the amount of energy that are available to create vibration is considerable and the structural members are relatively more complaint. In order to determine the safe operation of OTSGs, these vibrations problems must be investigated.

The availability of powerful numerical simulation techniques will certainly be of benefit to the field and, as it has proved in other industries (Charles and Baukal, (2003)). The progress towards increasing efficiency and reliability of the equipment can be achieved only through the use of more advanced numerical simulations (Charles and Baukal, (2012)).

Simulation and computer assisted engineering services are not sufficiently developed for satisfying the current needs of producers. Improvements in the

modelling methodologies to make them faster, more reliable and efficient for solving large problems are necessary to establish the producers to adopt and deploy these tools widely. The development of such tools and approaches gives a competitive advantage in the marketplace, and will help producers meet production, financial and HSE goals on a more stringently regulated industry.

Computational Fluid Dynamics (CFD) has become an accepted tool to help in the design and operation of oil and gas industry equipment. More recently, CFD has also found increasing application in the analysis of combustion equipment, such as industrial burners. In particular, CFD models are valuable assets for OTSG designers to study the efficiency in steam generation (Charles and Baukal, (2012)).

In comparison with empirical techniques, CFD would substantially reduce the total cost and processing time. However, CFD model development for such a complex equipment is challenging and requires deep understanding of physics as it simultaneously deals with the fields of combustion, heat transfer and phase change. to perform the CFD analysis in a timeframe compatible with the design and engineering process on such large and complex models, powerful computers are an indispensable requirement.

Singha and Forcinito (2018) proposed a methodology to reduce emission from a staged combustion burner in a typical OTSG. They produced a characterization map of the combustion system which was useful as a guideline towards efficient optimization of the OTSG during a field testing. Singha and Forcinito (2018) reached the conclusion that the CFD can minimize the number of experiments you need to

characterize a burner and in a particular case they succeeded in eliminating Flue-Gas Recirculation (FGR). E. Askari et. al. (2020) simulated and validated a 3D CFD model coupling combustion side inside the furnace and the steam generation inside the radiant and convection tubes through a typical Once-Through Generator (OTSG).

The present work outlines a CFD model development of an experimental combustor to predict NO<sub>x</sub> formation. This study also investigates the combustion induced acoustical waves as well as their propagation inside an experimental pre-mixed combustor. Initially combustion CFD simulations were performed using OpenFOAM to predict flow and temperature field and following that a NO<sub>x</sub> formation model and Large Eddy Simulation model were carried out in attempt to predict the NO<sub>x</sub> concentration and combustion-induced acoustical waves. The present research intends to serve as a typical case and aims to provide the detailed flow behaviour inside the combustor and NO<sub>x</sub> concentration.

### **BRNO Semi-Industrial Combustor**

In order to further validate the proposed combustion methodology as well as the NO<sub>x</sub> solver, the experimental results published for the semi-industrial combustor developed and constructed at the Brno University of Technology shown in Figure 1 was considered for the analysis conducted in this section (Belohradský & Kermes, 2012; JIRÍ VONDÁL, 2012; Kermes & Bělohradský, 2013).



Figure 1: Brno Semi-Industrial Combustor

In this unit, the combustion reactions are promoted by a two-staged burner, which is schematically represented in Figure 2.

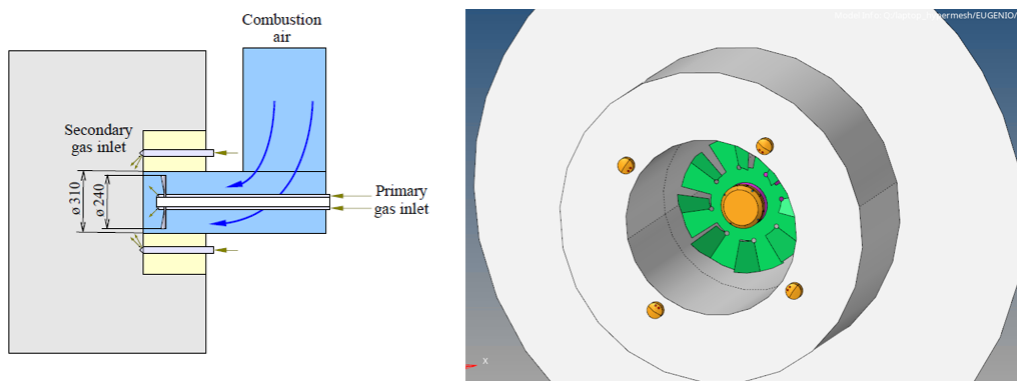


Figure 2: Schematic Representation of the Staged Burner (JIRÍ VONDÁL, 2012)

In the burner, the natural gas fuel is split and fed to combustor chamber through two different stages. The primary nozzle head consists of a set of 8 nozzles of 2.6 mm in diameter (green) and another of 4 nozzles with 3 mm in diameter (blue) as shown in Figure 3.

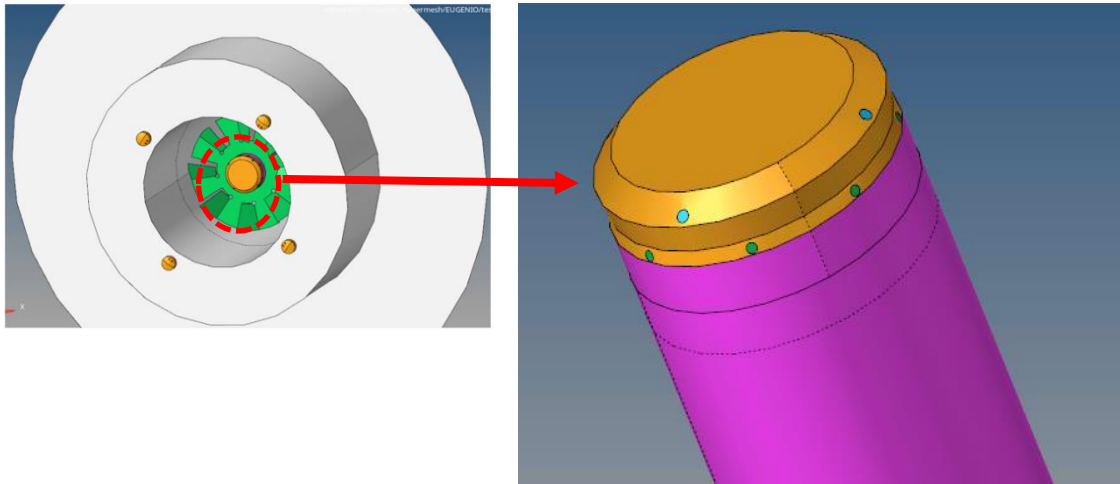


Figure 3: Primary Nozzle Head

The first set of nozzles directs part of the primary fuel stream perpendicular to incoming air flow at the base of flame holder, which maintains the flame stable and attached to the burner. The remaining of primary fuel is released by the second set of nozzles, and it is immediately ignited by the incoming hot combustion gases, whose combustion maintains the core of the flame at relatively high temperature so that the combustion process can be sustained during the operation.

At the same time, the remaining natural gas is fed to four secondary stage guns placed at the burner tile to reach the design firing rate, which is shown in Figure 4.

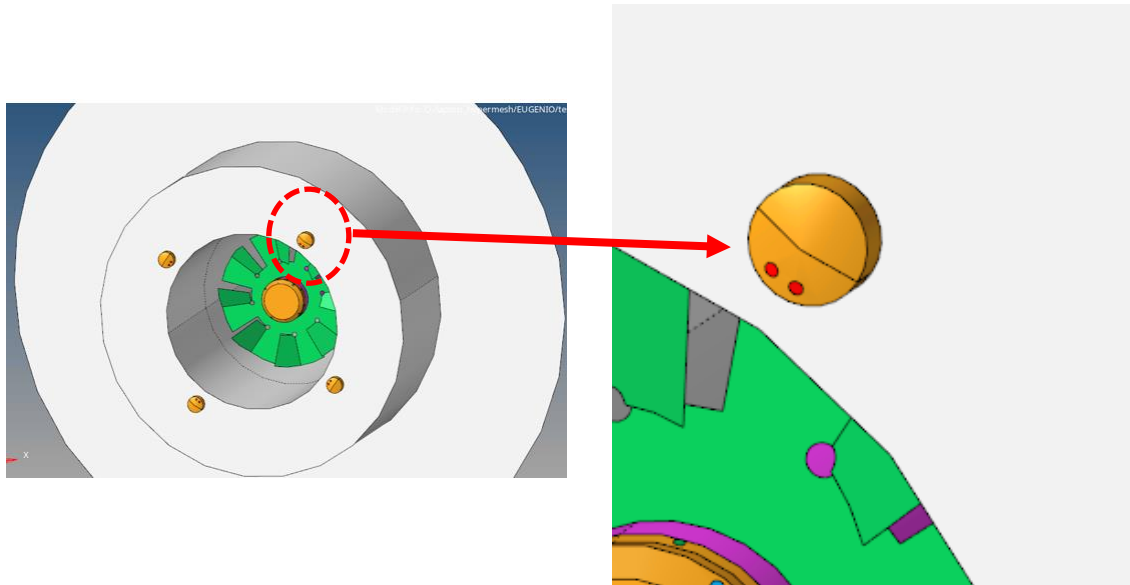


Figure 4: Secondary Stage Gun

Each of those guns contain two nozzles of 3.3 mm in diameter, which can be positioned at different angles relative to the burner axis. Additionally, the burner design allows to move these staged guns radially and axially to study the effect of its positioning on the burner performance. The incorporation of the secondary stage in this burner result in two major effects in the combustor operation. First, as the high-speed fuel jet from the secondary nozzles impinges the lateral vicinity of the flame, recirculation zones are formed around the flame. The rotating motion of the fluid within these recirculation zones draw hot combustion gases from the surrounds towards the flame, which locally dilutes the reacting mixture. Such mixing effect reduces the overall flame temperature and local nitrogen composition, and consequently, the rate of formation of NO<sub>x</sub> compounds is slowed down.

The fresh combustion air is fed to the unit through a wind tunnel connected to the annular region of the burner. Before the air is mixed with primary fuel, it crosses the flame holder, which is fitted with blades positioned at a specified angle. By

interacting with these blades, a swirling motion is induced in the air flow. This is desirable to enhance the turbulent mixing of reactants at the combustion zones.

The set of necessary operating conditions to impose the proper boundary conditions in the CFD simulations is given in Table 1.

Table 1: Operating Conditions for Brno Semi-Industrial Combustor

<b>Process Parameter</b>	<b>Value</b>
Firing Rate (kW)	745.7
Methane Mass Flow Rate (kg/s)	0.01486
Air Mass Flow Rate (kg/s)	0.289
Fuel Inlet Temperature (°C)	20.11
Air Inlet Temperature (°C)	19.23
Mass Flow Rate at Primary Stage (kg/s)	3.84x10 <sup>-3</sup>
Mass Flow Rate at Secondary Stage (kg/s)	1.10x10 <sup>-2</sup>

The combustion section is equipped with 7 independent lateral cooling chambers to absorb the heat released by combustion reaction. In these chambers, water is used as the cooling medium. According to (JIRÍ VONDÁL, 2012), the average wall temperature of each chamber is 80 °C, and thereby, this value was used as fixed temperature boundary condition for those walls.

Figure 6 shows the computational mesh generated based on the geometry for the Brno semi-industrial combustor.



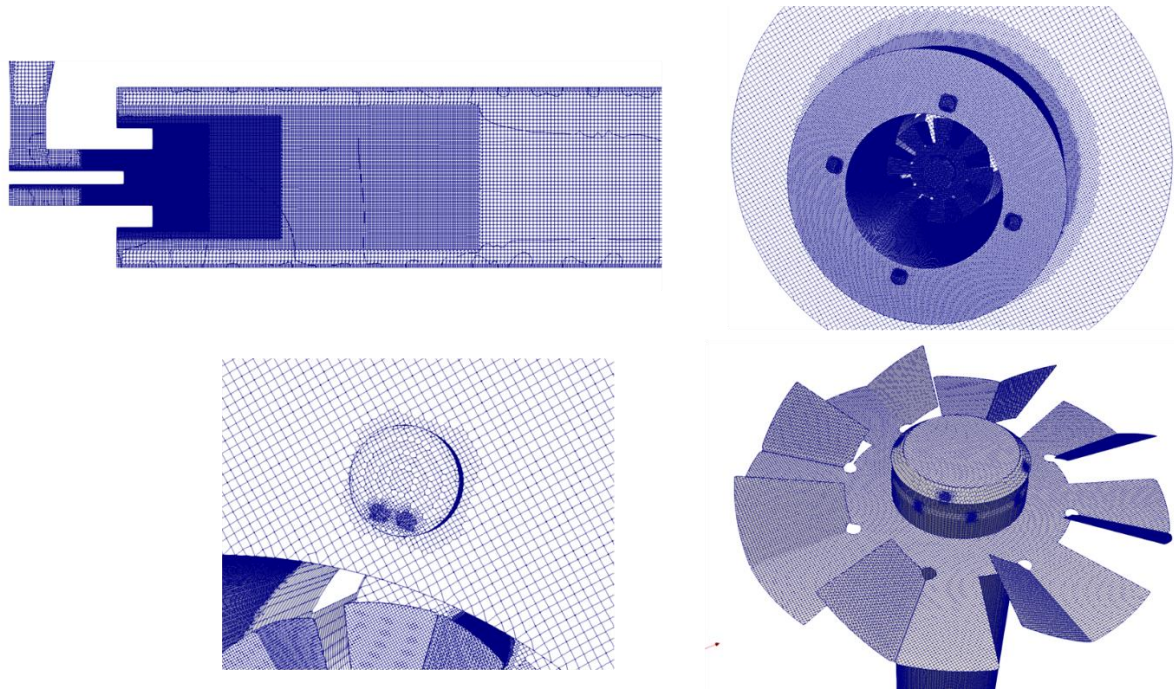


Figure 5: Computational Mesh for Brno Semi-Industrial Combustor

The total number of cells in the mesh is approximately 7 million. Local refinement was applied at regions around the primary and secondary nozzles to properly resolve the flow conditions at those regions. Furthermore, additional refinement was applied at the center of the combustion chamber to properly capture the flame characteristics and accurately compute the reactions rates. Finally, the flame holder is modeled as a zero-thickness wall, which significantly reduced size of the mesh since fine mesh was not required to resolve the small thickness of the holder. The solver configurations described in Table 2 were used to proper modeling of combustion process in the Brno semi-industrial combustor.

Table 2: Solver configurations used for the BRNO combustor simulation

<b>Physics</b>	<b>Sub-model</b>
Turbulence	SST k- $\omega$
Turbulence-Chemistry Interaction	EDM/EDC v2005
Radiation Model	f <sub>v</sub> DOM with 16 rays
Combustion Mechanism	Infinitely Fast Chemistry/Two-Step Westbrook Mechanism

In our research studies conducted at AP Dynamics, it was found out that the SST k- $\omega$  model is the best turbulence model to conduct steady-state combustion simulations. Moreover, this model is also the most suitable one to correctly predict the turbulence effects of swirling flows. As for the pilot-scale OTSG simulation, numerical stability was achieved by setting the under-relaxation factors for velocity and pressure to 0.3 and 0.6, respectively, while the factors for other variables were incremented from 0.4 to 0.6 as the simulation progressed. Finally, the results obtained using EDM and EDC v2005 are compared in this case to assess their performance to describe the turbulence-chemistry interactions. For the EDC case, the two-step Westbrook reaction mechanism was used to compute the reaction rates.

Figures 6 and 7 compare the time-averaged temperature and velocity profiles, respectively, obtained from the EDM and EDC models.

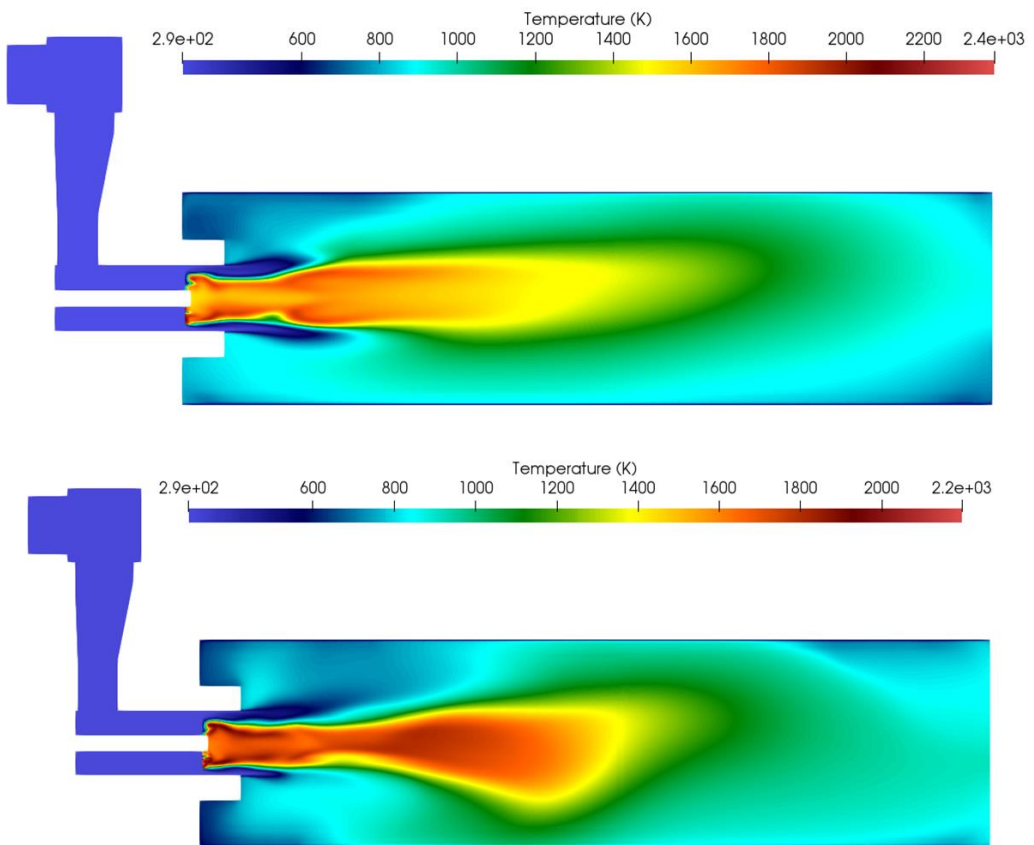


Figure 6: Time-Averaged Temperature Profiles obtained from EDM (Top) and EDC (Bottom)

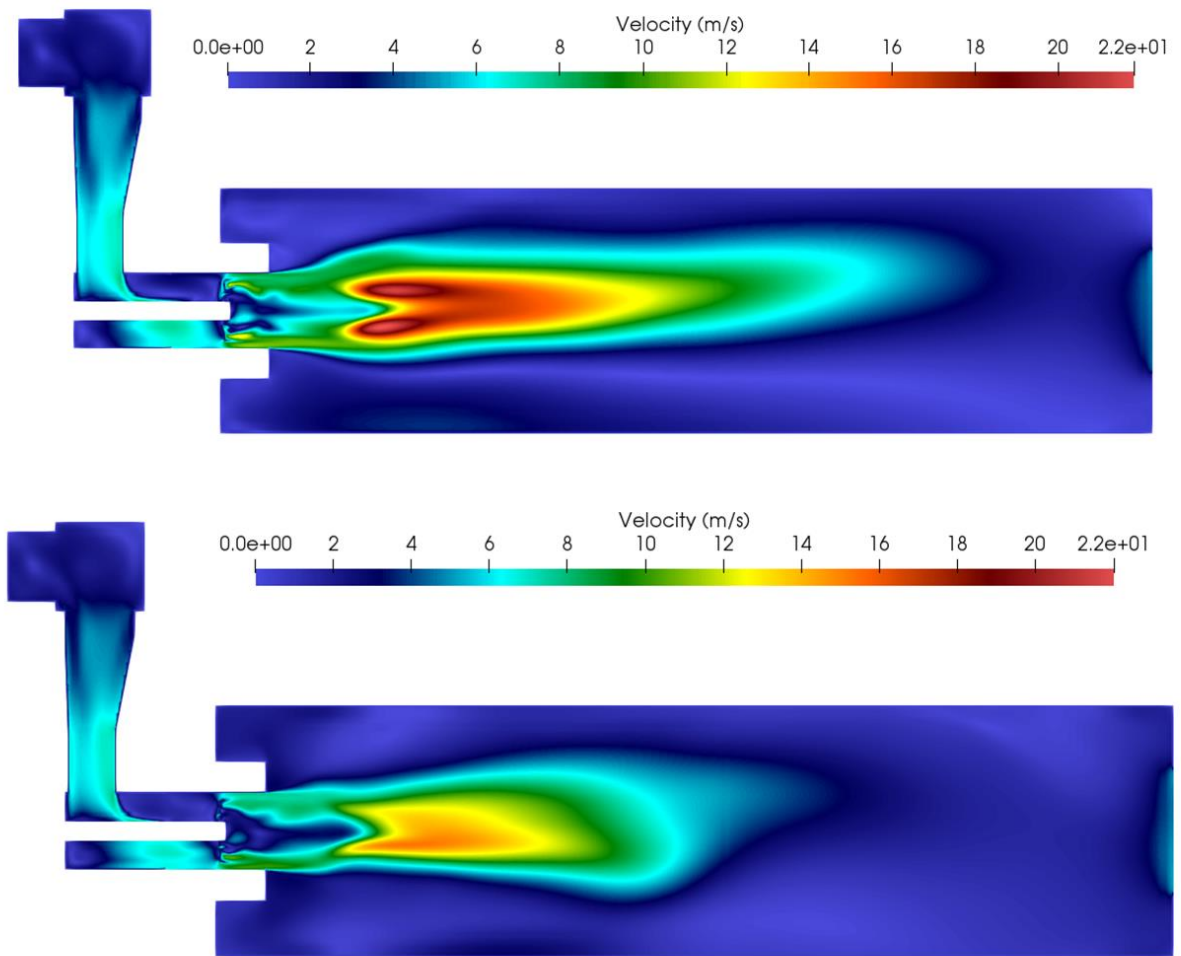


Figure 7: Time-Averaged Velocity Profiles for EDM (Top) and EDC (Bottom)

It can be observed that the flame is not symmetrical for both cases. The asymmetry is related to the strong recirculation zone formed at the bottom of the combustor. This behavior can be better visualized by using a vector plot along with the velocity contour in Figure 8.

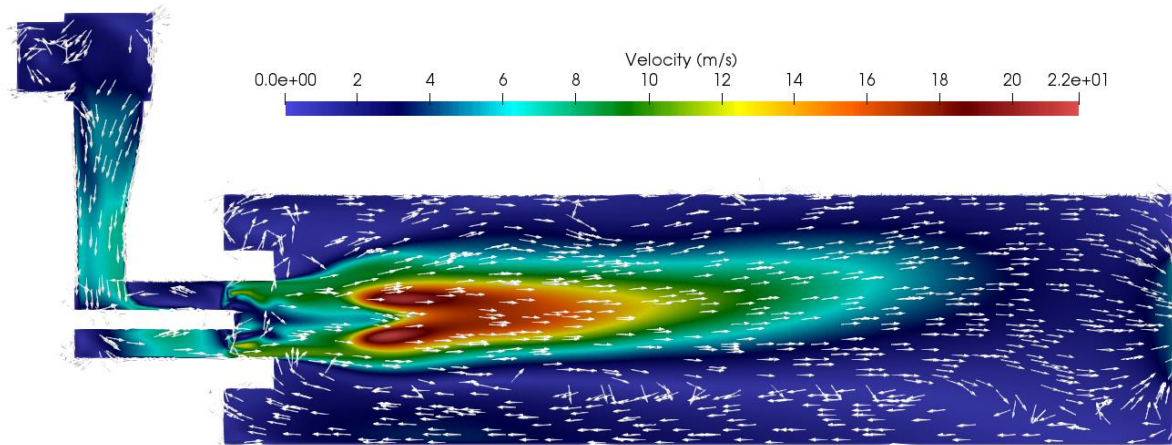


Figure 8: Vector Plot for the Brno Semi-Industrial Combustor

Moreover, this recirculation region induces a more uniform temperature distribution underneath the flame, which also indicates a dilution effect due to the mixing between the hot combustion gases and incoming cold air. Finally, the high-speed region observed inside the high temperature zone is related to combustion of the secondary fuel jets impinging the flame at that location.

In Table 3 3, the simulated heat flux results for each section are compared with the corresponding experimental and Fluent values reported by (JIRÍ VONDÁL, 2012). It is important to note that the fluent results reported were obtained from transient simulations since it was claimed that strong unsteadiness was observed in flow during operation of the combustor.

From Table 3, it can be observed that the heat fluxes obtained from the simulation are in well agreement with the experimental and Fluent values reported by (JIRÍ VONDÁL, 2012). However, it can be observed strong overprediction of the flux at the cooling chambers located in the mid-section of the combustion chamber. These

deviations can be attributed to the constant temperature imposed at boundaries representing the walls of each cooling chambers. Although strong mixing of the cooling water takes place within these chambers, there are indication that the presence of temperature gradients in the cooling water would possibly lead to more heat absorption. Additionally, significant uncertainties in the emissivity factors were also reported by (JIRÍ VONDÁL, 2012), which also might be further contributing to overprediction of the heat fluxes. Finally, some unsteadiness induced by the combustion plays an important role in the fluid dynamics and heat transfer mechanisms taking place in the system. Therefore, since a steady-solver has been used to conduce the simulation in OpenFOAM, numerical errors can be also affecting the simulation convergence as can be observed in Figure 9.

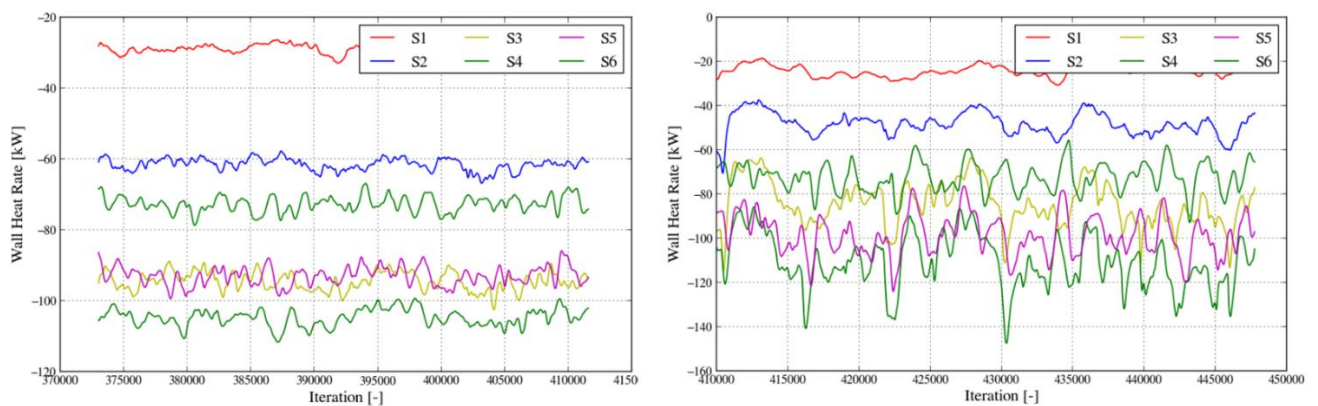


Figure 9: Variation of the Heat Flux per Iteration for the cases using EDM (left) and EDC (right)

It can be observed that the fluctuations are more intense in the case using the EDC with two-step combustion mechanism. In fact, convergence issues for combustion simulations using EDC have been reported in the previous report. Therefore, it is likely that the solution for the model using EDC is not entirely converged, which explains why the averaged velocity and temperature profiles have a blunter profile. On the other hand, the combustion simulation using EDM appears to have converged



to statistical steady state. Although the effect of unsteadiness might be affecting the convergence of the simulations, the comparisons presented in Table 3 still indicates a good agreement with the experimental values.

Table 3: Comparison of the Heat Flux Results for Each Cooling Section in kW/m<sup>2</sup>

Cooling Section	Experimental	OpenFOAM EDM	OpenFOAM EDC	Fluent Transient
1	17.25	18.98	15.06	17.2
2	25.57	37.63	32.41	28.6
3	40.17	58.49	57.58	39.7
4	46.41	64.05	74.10	45.2
5	47.87	57.09	63.68	45.1
6	42.33	47.19	45.66	41.6
7	31.4	26.95	27.36	36.5

As a last step, the averaged profiles for temperature, velocity, and compositions were used to compute the NO<sub>x</sub> composition of the flue gas leaving the combustion chamber using the customized steady-state NO<sub>x</sub> solver, which results are presented in Table 4.

Table 4: Validation of the Steady-State NO<sub>x</sub> solver for the BRNO Combustor Case

	Experimental	Simulated
NO <sub>x</sub> (ppm)	55	47.95

The NO<sub>x</sub> results obtained from the CFD simulation is in good agreement with the reported experimental value. The slight deviation can be related to two possible sources of uncertainty. The first possible source is the accuracy of the data acquisition equipment used to measure the NO<sub>x</sub> experimentally. It is well-known that the composition measurements can be affected by inaccuracy when the measured concentrations are very low. The second possible source is related to the

accuracy of the kinetic model used to compute the rates of NO<sub>x</sub> formation. Although, the used mechanism is very well validated in literature, the kinetic parameters are estimated using experimental data obtained for given range of pressure, temperature, and conversion. Consequently, using the same model for other conditions might increase the numerical errors and affect the results from the model. However, the results show that the predictions made by CFD model can still be reliable to make decisions related to the burner design as well as find the optimum conditions to run the combustor so that the NO<sub>x</sub> emissions are minimized.

### **LIMOUSINE Pre-mixed Combustor**

In this section, combustion simulations are conducted to assess the possibility of using computation fluid dynamics as tool to study the controlling mechanism related to combustion-induced vibrations. For this task, a pre-mixed combustor developed for the LIMOUSINE consortium is simulated since experimental and simulation results are widely reported in literature for this equipment (Mina Shahi, 2014). Figure 10 shows a schematic representation of the experimental combustor.



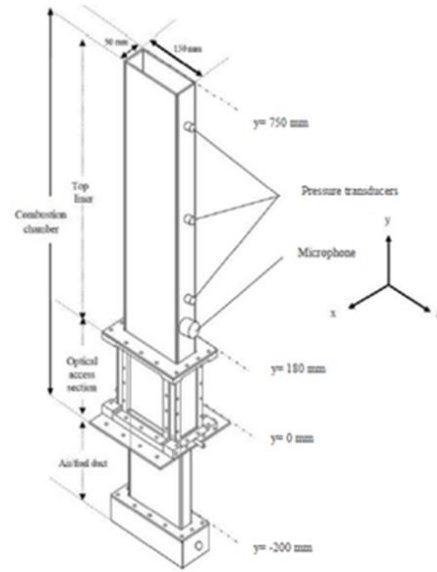
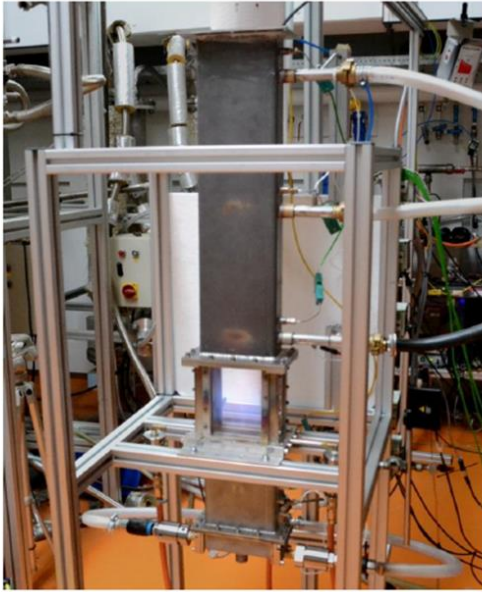


Figure 10: LIMOUSINE Pre-mixed Combustor (Mina Shahi, 2014)

The unit is vertical, and air is supplied from nozzles located at the bottom of the air duct, which is located 220 mm upstream from the triangular bluff body burner. A schematic representation of the burner is shown in Figure 11.

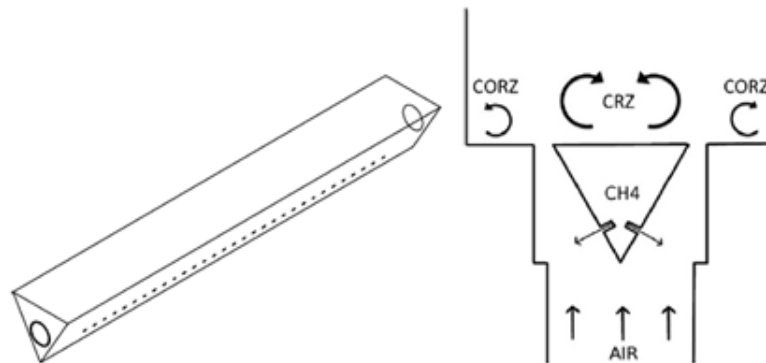


Figure 11: Triangular Bluff Body Burner (Mina Shahi, 2014)

The burner contains 62 holes equally distributed along two faces of its triangular body shape through which methane is injected into the incoming air stream. Each

hole has 2 mm in diameter. Upon flow separation, the pre-mixed air-fuel stream is ignited. Recirculation zones are formed at two different locations around the vicinity of the burner. The first one is behind the bluff-body, where the flow separation causes a turbulent wake, which increases the turbulent mixing between reactants and hot combustion gases. Due to difference in local flow velocities, recirculation zones are also formed at the two corners of the combustor. The presence of these two recirculation zones is important to keep the flame stable for a wide range of operating conditions. When operating at very high Reynolds number, the chemical time scale become large compared to that for turbulence mixing. Consequently, flame instability can be observed under these conditions since the reactants do not spend enough time in the reaction zone.

The downstream combustion zone is 720 mm high. Since the width of the unit (150 mm) is much larger than its thickness, the geometry was simplified by using cyclic AMI periodic boundary condition on a model of a slice of the combustor as shown in Figure 12.

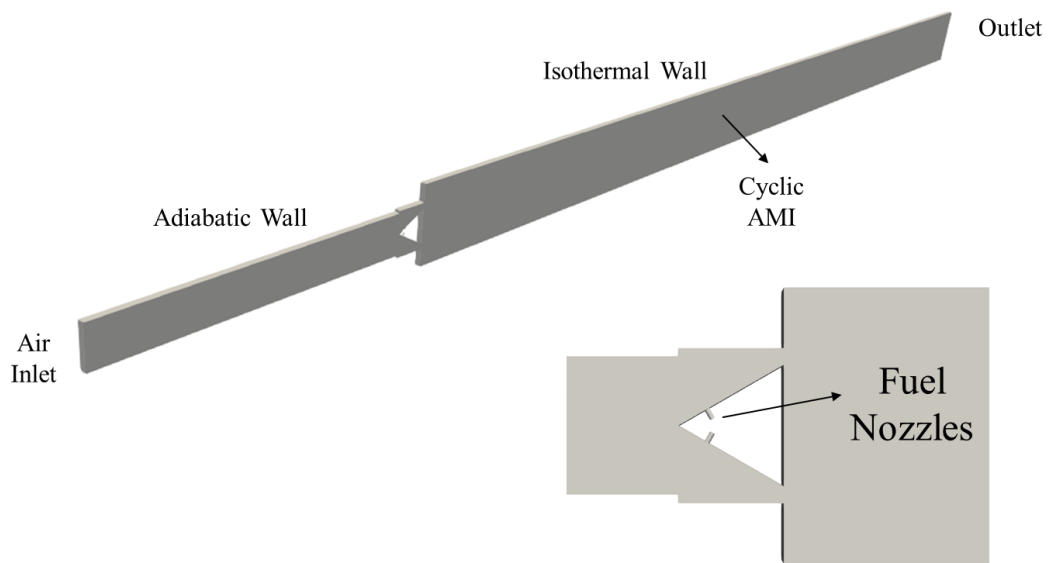


Figure 12: Periodic Geometry for the LIMOUSINE combustor

Such simplification allows the use of large-eddy simulation for this case without significant increase in computing time. Also, the slice is made ensure a fuel nozzle each side of the triangular burner.

The computational mesh generated for the LIMOUSINE combustor is shown in Figure 13.

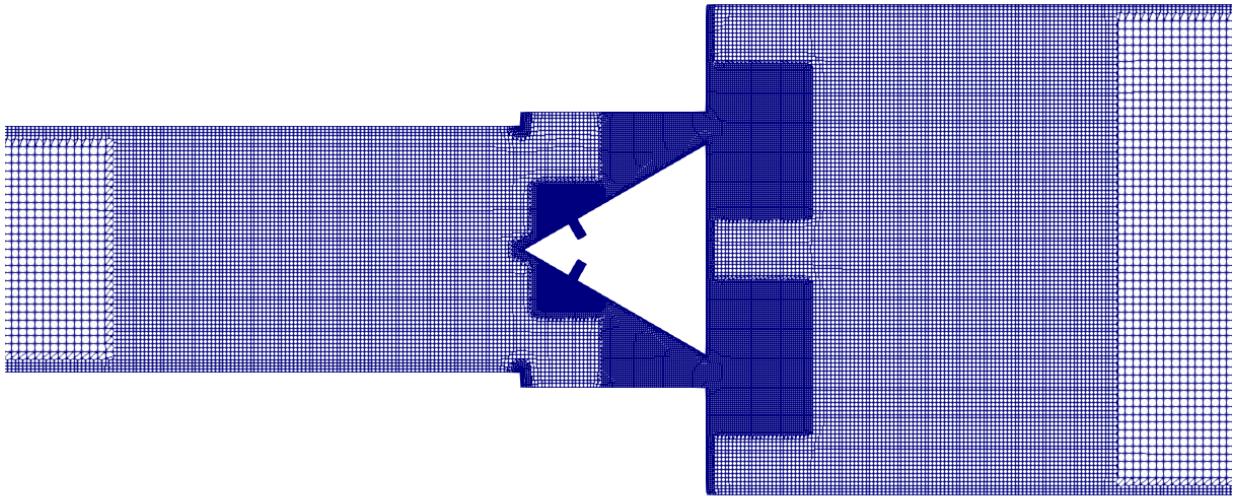


Figure 13: Computational mesh for the LIMOUSINE combustor

The generated mesh contains approximately 7 million cells. Additionally, refinement zones were placed around the nozzles and the expansion zones to properly resolve the flow and recirculation zones. Finally, the size of the smallest cell was selected to resolve at least 70% of turbulent kinetic energy and satisfy a courant number of 0.2, which are standard recommendations to properly conduct LES simulations.

The following solver configurations described in Table 5 were used to simulate of combustion process in the LIMOUSINE combustor.

Table 5: Solver configurations used for the LIMOUSINE combustor simulation.

<b>Physics</b>	<b>Sub-model</b>
Time-step	$1 \times 10^{-6}$ s
Turbulence	LES WALE/SST k- $\omega$ SAS
Turbulence-Chemistry Interaction	EDC v2005
Combustion Mechanism	One-Step Westbrook Mechanism

Two turbulence models were tested in this case. For the LES simulation, the Wall Adapting Local Eddy-Viscosity (WALE) was applied since it is simple and capable to predict the flow conditions at the near-wall region. Although LES turbulence models are more suitable to predict flow-induced oscillations compared to URANS, they require large computing times due to the fine mesh and small computing time requirements. To overcome this drawback, the same CFD model is solved using the Scale Adaptive Simulation (SAS) SST  $k-\omega$  model. This is a hybrid turbulence model that uses the LES formulation only at regions where the mesh is fine enough to resolve the eddies, and URANS at regions where the mesh is relatively coarse. Therefore, by applying this method, the finer mesh regions close to the burner are well-resolved and simulated using LES whereas the downstream portion is modelled as URANS. The goal is to compare these two methods in terms of accuracy and computing time.

According to the studies carried out by (Mina Shahi, 2014), combustion-induced oscillations occur due to a feedback mechanism coupling the following phenomena:

- Formation of turbulent eddies due to the turbulence flow occurring in the combustor;
- Increase in local temperature due to heat released by the exothermic combustion reaction;
- Changes in local density due to the increase in temperature, which enhances the turbulence due to the buoyancy effects.

Therefore, the CFD model must be capture these coupling effects to be considered an effective tool to study combustion-induced vibrations, and to be used to propose design solutions that can mitigate this issue. Figure 14 and Figure 15 show the

temperature and velocity profiles obtained from both LES and SAS simulations, respectively, at the last time-step.

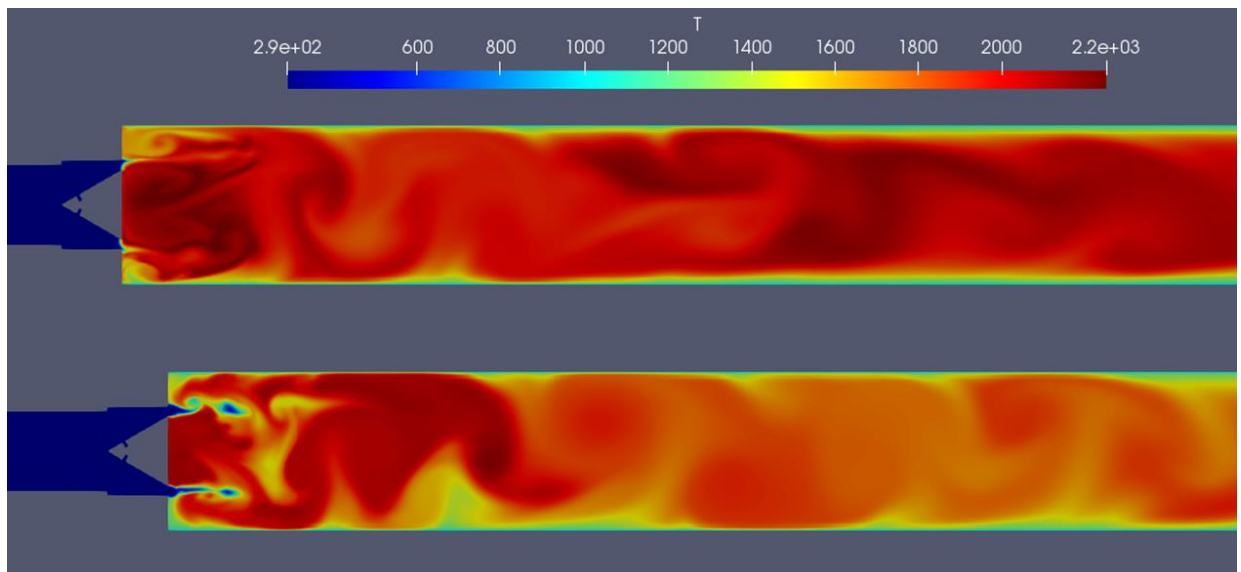


Figure 14: Temperature profile obtained using SAS SST  $k-\omega$  (top) and LES (bottom) turbulence models

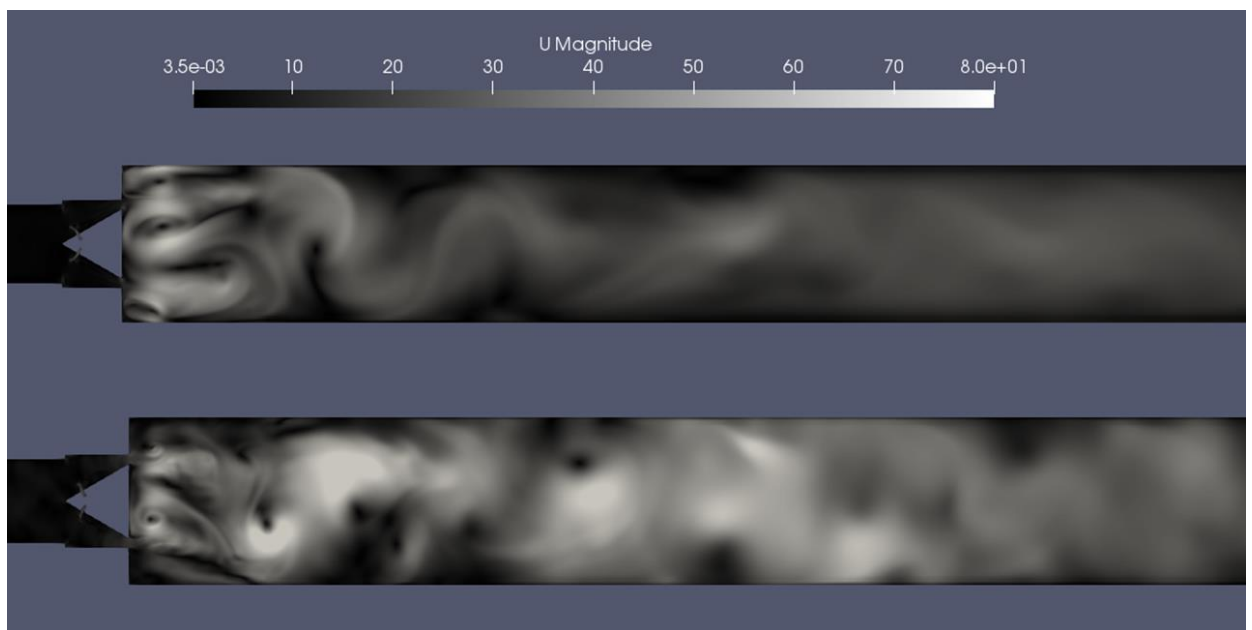


Figure 15: Velocity profile obtained using SAS SST  $k-\omega$  (top) and LES (bottom) turbulence models

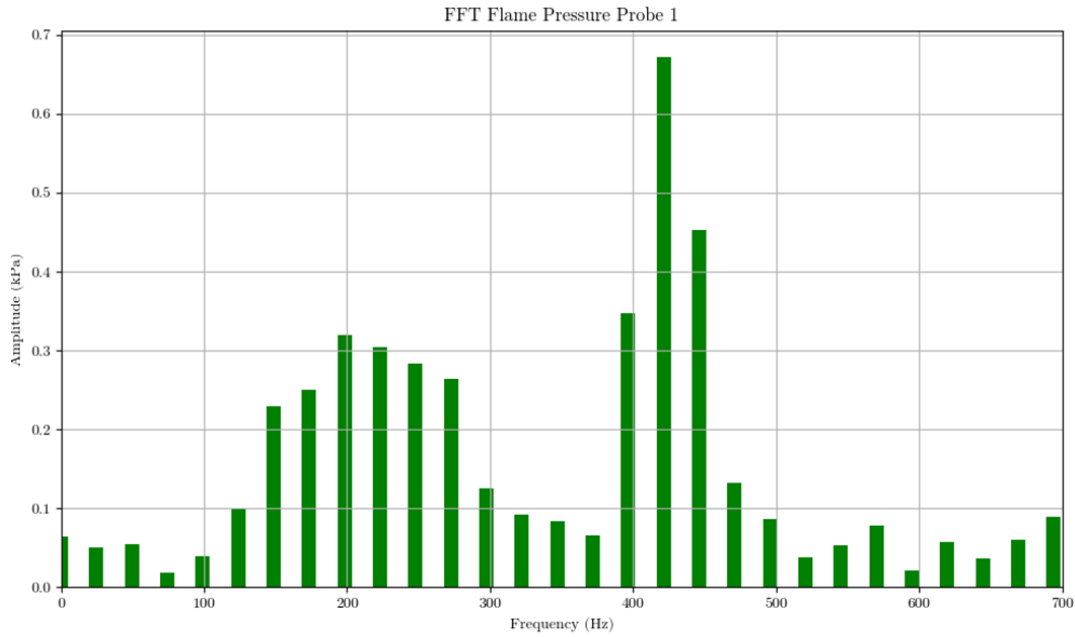
It can be observed that the LES simulations provided good resolution of the turbulence eddies generated by the flow separation and recirculation zones near the

burner. In the case of the hybrid LES turbulence model, the resolution is smoother due to the time-averaging component of the URANS formulation, whose effect is more pronounced in the profiles further downstream as the mesh becomes coarser. For post-processing and validation purposes, pressure data was recorded during the simulation using pressure probes placed at three different locations downstream from the burner as indicated in Table 6.

Table 6: Pressure Probe Location (Mina Shahi, 2014)

<b>Probe</b>	<b>Distance from the Burner (mm)</b>
1	20.4
2	45.4
3	70.4

The pressure data was recorded every  $1 \times 10^{-5}$  second to avoid aliasing effects, and the dominant frequencies in the signals were computed through fast-Fourier transform analysis (FFT). Figure 16 provides a comparison of the experimental and simulated values for frequencies computed from the data collected at the first probe using fast-Fourier transform (FFT).



	First Peak	Second Peak
Experimental	185 Hz	390 Hz
LES	169 Hz	415 Hz
Hybrid RANS	198 Hz	422 Hz

Figure 16: Comparison between experimental and simulated frequencies for probe 1

It can be observed that both LES and hybrid RANS turbulence models were able to capture the correct first and second peak frequencies related to the combustion-induced oscillations. Slightly higher discrepancy was found for hybrid LES method since some time-averaging is still carried out due its formulation. However, it was noted that the hybrid-LES turbulence model was four times faster compared to the full LES simulation, which is a significant improvement that proves its potential to conduct this type of analysis for designing and troubleshooting of industrial combustors. Finally, Figure 17 shows the time history of the pressure signals collected at the three different probes in an interval of 0.05 seconds.



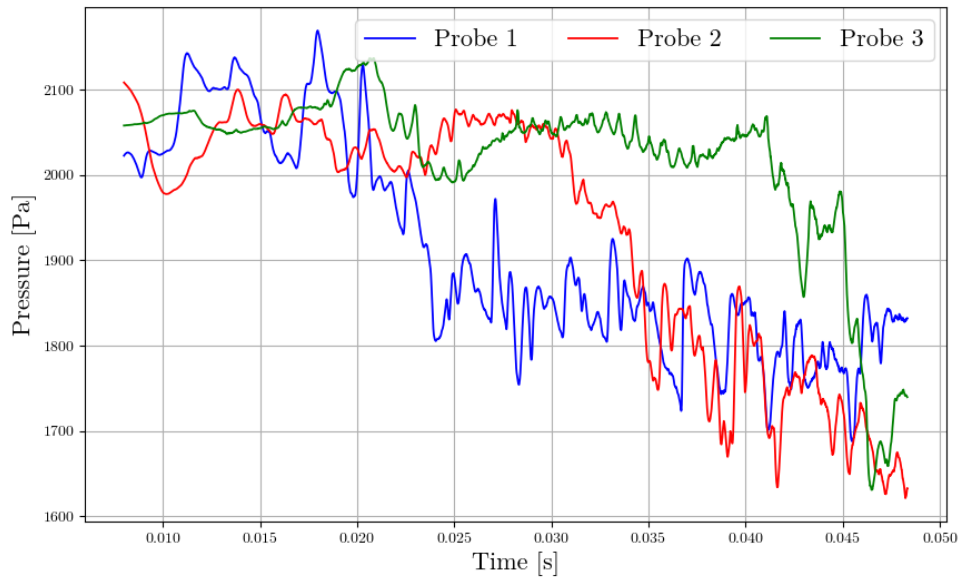


Figure 17: Time history of the pressure and temperature at three different probes

Pressure changes occur faster at regions closer to the burner since turbulence eddies are mostly formed in that region. From data extracted from the probes located farther downstream, it can be noted that there is time-lag between the pressure signals, which is related to the time required for the turbulence eddies to travel to those probe locations. Such behaviour shows the coupling between the turbulence and combustion mechanisms.

## **Conclusion**

In the framework of our current research, further validation of the CFD methodology was carried out by conducting additional simulations for the operation of a semi-industrial combustor, for which experimental data in terms of NO<sub>x</sub> emissions and heat fluxes were available from literature. A customized solver was used to conduct the NO<sub>x</sub> calculations considering steady state operation, which significantly reduced the computing time to acquire results. Based on the comparisons made with experimental data, the simulated results were in very good agreement with experimental values, even though some unsteadiness in the flow has been reported.

The application of CFD models to describe combustion-induced oscillations was investigated. For this task, a simple case involving partially premixed combustion taking place in a vertical combustor was taken into consideration. Since capturing the oscillations in the flow was important, a LES turbulence model was used to simulate the case. Additionally, the results were compared to those obtained by applying a hybrid LES/URANS turbulence model, which only uses the LES formulation at specific regions of the computational domain. The results from both methods showed good agreement with the experimental frequency data reported in literature. It was also shown that although effect of time-averaging of the turbulent eddies were still observed in profiles obtained from the hybrid LES method, the results were nearly same as those reported for the full LES model. Also, the time required to run the simulation using the hybrid model was four time faster compared to the full LES approach. Therefore, it is proven that the SAS turbulence

model can be a good candidate to be used in engineering analysis and understand the underlying mechanisms governing the combustion-induced oscillations.

### **Acknowledgments**

The authors would like to thank International Research Activities by Small and Medium-sized Enterprises (IraSME) which financially supported this study. The authors would like to sincerely thank Eugenio Turco Neto for his contribution during the time he was at AP Dynamics.

## References

A. Singha & M. Forcinito, 2016, *Thermo-Mechanical Analysis of a Refractory - Root Cause Analysis*, 2016 NAFEMS Americas Conference, Seattle, Washington.

A. Singha and M. Forcinito, 2018, *Emission Characteristic Map and Optimization of NO<sub>x</sub> in 100 MW Staged Combustion Once-Through-Steam-Generator (OTSG)*, ARFC Industrial Combustion Symposium, Salt Lake City, USA

A. Singha and M. Forcinito, 2019, *Modelling Different Aspects of Once Through Steam Generators*, NAFEMS, Quebec City, Canada

Belohradský, P., & Kermes, V. (2012). *Experimental Study on NO<sub>x</sub> Formation in Gas- staged Burner Based on the Design of Experiments*, Chemical Engineering Transactions, 29, 79–84 SE–Research Articles.

Diez L, Cortes C, Artauzo I, Valero A, 2001. *Combustion and Heat Transfer Monitoring in large Utility Boilers*, International Journal of Thermal Sciences, 40:489-496.

E. Charles & Jr. Baukal, 2003, *Industrial Burners Handbook*, CRC Press

E. Charles & Jr. Baukal 2012, *The John Zink Combustion Handbook*, CRC Press

E. Askari, E. Turco Neto, A. Maesen, M. Forcinito and L. Fitschy, 2020, *3D CFD Model Development and Validation for Once-Through Steam Generator (OTSG): Coupling Combustion, Heat Transfer and Steam Generation*, ARFC Industrial Combustion Symposium, Virtual, USA

Kermes, V., & Bělohradský, P. (2013). *Biodiesel (EN 14213) heating oil substitution potential for petroleum based light heating oil in a 1 MW stationary combustion facility*. Biomass and Bioenergy, 49, 10–21.

M. Shahi. (2014). *Modeling of Complex Physics and Combustion Dynamics in a Combustor with a Partially Premixed Turbulent Flame*. University of Twente

Turns, S. B., 2012. *Introduction to Combustion: Concepts and Applications*, McGraw Hill.

Versteeg H. K., Malalasekera W. 1995. *An Introduction to Computational Fluid Dynamics – The Finite Volume Approach*, Longman Scientific and Technical.

JIRÍ VONDÁL. (2012). *Computational Modeling of Turbulent Swirling Diffusion Flames*. Brno Research of Technology.